

Evaluation of equilibrium parameters of the anatase/aqueous electrolyte solution interface by introducing surface potential data

Tajana Preočanin^{a,*}, Wladyslaw Janusz^b, Nikola Kallay^a

^a Laboratory of Physical Chemistry, Department of Chemistry, Faculty of Science, University of Zagreb, Horvatovac 102a, 10001 Zagreb, Croatia

^b Department of Radiochemistry and Colloid Chemistry, Maria Curie-Skłodowska University, Pl. M.C. Skłodowskiej 3, 20-031 Lublin, Poland

Received 7 July 2006; received in revised form 3 October 2006; accepted 7 October 2006

Available online 12 October 2006

Abstract

The single crystal anatase electrode (SCrE) was used to measure the inner surface potential (φ_0) at the anatase/aqueous electrolyte interface as a function of pH. Measurements were performed in sodium perchlorate and sodium chloride aqueous solutions. Absolute values of the surface potential were calculated from electrode potentials using the electrokinetic isoelectric point as the point of zero potential. The slope of φ_0 (pH) function, with respect to pH, was found to be lower than the Nernstian. These results were accompanied with surface charge density and electrokinetic potential data and were interpreted simultaneously on the basis of the Surface Complexation Model. Both 1-pK and 2-pK mechanisms were employed. Data in the acidic region were interpreted since they were more reliable. Simultaneous interpretation of three sets of data enabled calculation of surface concentrations of all species, and thus thermodynamic equilibrium constants and the inner layer capacitance for each pH value separately. It was found that the equilibrium constants of surface protonation did not depend on the pH and the nature of the counterions, supporting the applicability of both 1-pK and 2-pK models. Thermodynamic equilibrium constants for association of perchlorate ions with positively charged surface groups did not change with pH, as expected, but the inner layer capacitance changed from 0.5 to 1.5 F m⁻² by increasing the pH. Chloride ions showed an increase in the association equilibrium constant with pH and a less pronounced increase of capacitance. The advantage of the applied procedure lies in the possibility of avoiding the model assumptions of the constancy of parameters describing the interfacial equilibrium. It was shown that the thermodynamic equilibrium constants of surface protonation are real constants as defined by the Surface Complexation Model. The capacitance, however, changes with pH and surface potential and its constancy is just an approximation introduced by necessity when only one set of experimental data, such as surface charge density is quantitatively interpreted.

© 2006 Elsevier B.V. All rights reserved.

Keywords: Single crystal electrode; Anatase; Surface potential; Surface Complexation Model; Electrical double layer; Ion association

1. Introduction

One of the important parameters affecting the interfacial equilibrium of metal oxide aqueous systems is the electrostatic potential at the inner plane of the Helmholtz interfacial layer (O-plane), i.e. the surface potential φ_0 [1]. This surface potential determines the activity coefficients of charged species bound directly to the surface [2]. Measurements of the surface potential were enabled by the development of metal oxide single crystal electrodes (SCrE). The work was initiated by construction of the ice electrode [3,4] and continued with the hematite electrode [5,6]. In this report, results obtained with a single

crystal anatase electrode will be presented. Usage of a single crystal avoids the problem of porosity of the metal oxide layer connected directly to a conductor (metal). It is obvious that a metal wire covered with metal oxide particles has, due to the porosity of the oxide layer, a response controlled by the redox process and the metal oxide solubility, rather than due to the surface potential developed by adsorption of ionic species. Surface potentials were evaluated from the measured electromotivities (values of the electromotive force) [7] of the cell consisting of a single crystal and a reference electrode by setting the zero value of φ_0 at the isoelectric point [5,6]. Surface potential measurements enable evaluation of the ratio of surface concentrations of unassociated negative and positive surface species. This is important information, because adsorption data provide only differences in their surface concentrations.

* Corresponding author. Tel.: +385 1 46 06 130/54; fax: +385 1 46 06 131.
E-mail address: tajana@chem.pmf.hr (T. Preočanin).

Measurements of the surface potential φ_0 , combined with the surface charge density σ_0 (obtained by potentiometric acid–base titrations of the metal oxide colloid suspension) and with electrokinetic potential data (ζ -potential) enable evaluation of singular values of concentrations of all active species at the interface, and thus direct calculations of the surface equilibrium constants and of the capacitance of the inner Helmholtz layer within the electrical interfacial layer (EIL) [8]. Such results are essential for a critical evaluation of theoretical models describing the interfacial equilibrium, and especially useful for interpretation of calorimetric acid–base titrations of metal oxide colloid suspensions where one should separate extents of protonation and deprotonation of neutral surface sites [9].

This article presents the results for the pH dependency of the surface potential of anatase in an aqueous environment containing two different electrolytes, sodium perchlorate and sodium chloride. It is expected that the magnitude of the slope of the $\varphi_0(\text{pH})$ function will depend on the nature of the counterions. The data on surface potentials were accompanied with the results of surface charge density and electrokinetic potential measurements.

It was shown by Westall and Hohl [10] that the data on surface charge density solely cannot distinguish between different variations of the Surface Complexation Models (SCM) and different assumed structures of EIL. The standard procedure for estimation of surface protonation and counterion association equilibrium constants, as well as of the electrical capacitances, involves fitting of experimental potentiometric acid–base titration data [11]. In such an interpretation, it is necessary to assume the constant value of the capacitance of the inner Helmholtz layer [12,13].

Association of counterions with oppositely charged surface groups is characterized by two parameters: the thermodynamic equilibrium constant (often called “intrinsic constant”) and electrical capacitance of the inner Helmholtz layer. The extent of counterion association is affected by the surface potential at the β -plane where centers of counterions are located, φ_β . Higher capacitance value will cause higher values of φ_β compared to φ_0 . Consequently, effectively smaller counterions, in the sense of the Bjerrum association theory [14,15], will exhibit higher affinity towards association at the surface both due to the higher thermodynamic association equilibrium constant and higher capacitance of the inner Helmholtz layer.

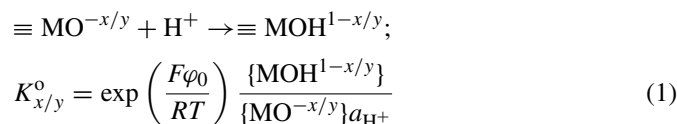
The aim of this article is to show how the surface potential data, along with surface charge and electrokinetic data, may serve in the interpretation of complex equilibrium within the interfacial layer. Both 1-pK and 2-pK mechanisms of the Surface Complexation Model were employed. In the interpretation, only the slip plane separation and total number of surface sites were estimated. The constancy of thermodynamic equilibrium constants will be tested and the possible pH dependency of the electrical capacitance will be examined.

2. Theory

Quantitative interpretation of equilibrium at the metal oxide/aqueous electrolyte interface is based on the SCM, assum-

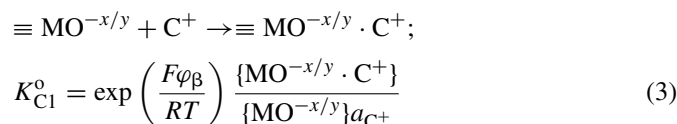
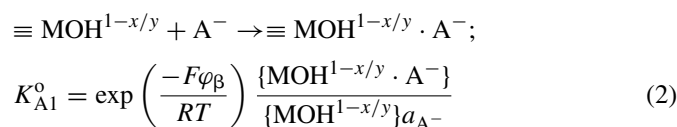
ing both 1-pK [16–18] and 2-pK [19,20] mechanisms of surface protonation, by taking into account the structure of EIL [8,21].

According to the 1-pK mechanism, surface equilibrium is described by one step protonation



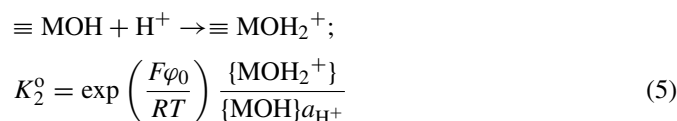
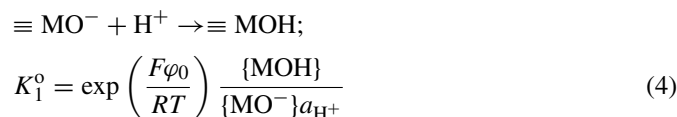
where curly braces denote surface concentration, $K_{x/y}^0$ the thermodynamic equilibrium constant of the corresponding surface reaction and φ_0 is the electrostatic potential affecting the state of charged surface groups $\equiv \text{MO}^{-x/y}$ and $\equiv \text{MOH}^{1-x/y}$. Charge numbers of surface groups ($-x/y$ and $1-x/y$) depend on the coordination of metal atoms in metal oxides [16]. For anatase, the values $x=1$ and $y=3$ are commonly used [17,22]. For interfacial species, activity is defined in terms of surface concentration so that the exponential term in Eq. (1) represents the ratio of activity coefficients of charged surface species [2].

Effective surface charge is reduced by association of anions A^- and cations C^+ with oppositely charged surface sites (reactions (2) and (3), respectively)



where $K_{\text{A}1}^0$ and $K_{\text{C}1}^0$ are thermodynamic equilibrium constants of the corresponding surface reactions and φ_β is the electrostatic potential affecting the state of associated counterions.

According to the 2-pK mechanism, amphoteric surface groups on the metal oxide surface undergo protonation and deprotonation depending on the pH. Here, the charging process will be represented by the two-step protonation



where K_1^0 and K_2^0 are thermodynamic equilibrium constants of the corresponding surface reactions, and φ_0 is the electrostatic potential affecting the state of charged surface groups $\equiv \text{MOH}_2^+$ and $\equiv \text{MO}^-$. According to the above formalism, K_2^0 is identical to the protonation equilibrium constant, while K_1^0 is equal to the reciprocal value of the deprotonation equilibrium constant.

Effective surface charge is reduced by association of anions A^- and cations C^+ with oppositely charged surface sites (reac-

tions (6) and (7), respectively)

$$\begin{aligned} &\equiv \text{MOH}_2^+ + \text{A}^- \rightarrow \equiv \text{MOH}_2^+ \cdot \text{A}^-; \\ K_{\text{A}2}^{\circ} &= \exp\left(\frac{-F\varphi_{\beta}}{RT}\right) \frac{\{\text{MOH}_2^+ \cdot \text{A}^-\}}{\{\text{MOH}_2^+\}a_{\text{A}^-}} \end{aligned} \quad (6)$$

$$\begin{aligned} &\equiv \text{MO}^- + \text{C}^+ \rightarrow \equiv \text{MO}^- \cdot \text{C}^+; \\ K_{\text{C}2}^{\circ} &= \exp\left(\frac{F\varphi_{\beta}}{RT}\right) \frac{\{\text{MO}^- \cdot \text{C}^+\}}{\{\text{MO}^-\}a_{\text{C}^+}} \end{aligned} \quad (7)$$

where $K_{\text{A}2}^{\circ}$ and $K_{\text{C}2}^{\circ}$ are thermodynamic equilibrium constants of the corresponding surface reactions, and φ_{β} is the electrostatic potential affecting the state of associated counterions.

Definition of the total surface concentration of active surface sites Γ_{tot} depends on the assumed mechanism, so that

$$\begin{aligned} \Gamma_{\text{tot}} &= \{\text{MOH}^{1-x/y}\} + \{\text{MO}^{-x/y}\} + \{\text{MOH}^{1-x/y} \cdot \text{A}^-\} \\ &\quad + \{\text{MO}^{-x/y} \cdot \text{C}^+\}; \quad 1\text{-pK} \end{aligned} \quad (8)$$

and

$$\begin{aligned} \Gamma_{\text{tot}} &= \{\text{MOH}\} + \{\text{MOH}_2^+\} + \{\text{MO}^-\} + \{\text{MOH}_2^+ \cdot \text{A}^-\} \\ &\quad + \{\text{MO}^- \cdot \text{C}^+\}; \quad 2\text{-pK} \end{aligned} \quad (9)$$

The model of the electrical interfacial layer postulates several layers and planes [21]. In the first plane, at the solid surface (0-plane), the surface charged groups are located. In the case of the 1-pK model: $\equiv \text{MOH}_2^{1-x/y}$ and $\equiv \text{MO}^{-x/y}$; for 2-pK model: $\equiv \text{MOH}_2^+$ and $\equiv \text{MO}^-$. This plane is characterized by the inner surface potential φ_0 . Centers of associated counterions are located in the β -plane characterized by the outer surface potential φ_{β} . The onset of diffuse layer is the d-plane with the electrostatic potential φ_d . Electrokinetic slip plane (s-plane) corresponds to the electrokinetic ζ -potential. These planes define three layers: inner (Helmholtz) layer between 0- and β -planes, outer (Helmholtz) layer between β - and d-planes, and diffuse layer that extends from the d-plane towards the bulk of the liquid medium. Diffuse layer may be divided in two parts, the immobile one that stays (or moves) together with the solid surface (the so-called hydrodynamically stagnant layer) and the mobile one that moves (or stays) together with the bulk of the liquid medium. These two parts of the diffuse layer are divided by the hydrodynamic slip or shear plane (s-plane) [8].

Surface charge density in the 0-plane (σ_0) also depends on the assumed charging mechanism

$$\begin{aligned} 1\text{-pK:} \quad \sigma_0 &= F \left[\left(1 - \frac{x}{y}\right) \{\text{MOH}^{1-x/y}\} \right. \\ &\quad + \left(1 - \frac{x}{y}\right) \{\text{MOH}^{1-x/y} \cdot \text{A}^-\} \\ &\quad \left. - \frac{y}{x} \{\text{MO}^{-x/y}\} - \frac{y}{x} \{\text{MO}^{-x/y} \cdot \text{C}^+\} \right] \end{aligned} \quad (10)$$

and

$$\begin{aligned} 2\text{-pK:} \quad \sigma_0 &= F(\{\text{MOH}_2^+\} + \{\text{MOH}_2^+ \cdot \text{A}^-\} \\ &\quad - \{\text{MO}^-\} - \{\text{MO}^- \cdot \text{C}^+\}) \end{aligned} \quad (11)$$

Surface charge density in the β -plane (σ_{β}) is related to surface concentrations of associated counterions by

$$\sigma_{\beta} = F(\{\text{MO}^{-x/y} \cdot \text{C}^+\} - \{\text{MOH}^{1-x/y} \cdot \text{A}^-\}); \quad 1\text{-pK} \quad (12)$$

and

$$\sigma_{\beta} = F(\{\text{MO}^- \cdot \text{C}^+\} - \{\text{MOH}_2^+ \cdot \text{A}^-\}); \quad 2\text{-pK} \quad (13)$$

The net (effective) surface charge density σ_s is related to the difference in surface concentrations of free positive and negative surface sites and is equal in magnitude but opposite in sign to “surface charge density of the diffuse layer” σ_d

$$\begin{aligned} \sigma_s &= -\sigma_d \\ &= F \left(\left(1 - \frac{x}{y}\right) \{\text{MOH}^{1-x/y}\} - \frac{x}{y} \{\text{MO}^{-x/y}\} \right); \quad 1\text{-pK} \end{aligned} \quad (14)$$

and

$$\sigma_s = -\sigma_d = F(\{\text{MOH}_2^+\} - \{\text{MO}^-\}); \quad 2\text{-pK} \quad (15)$$

According to Eqs. (1), (4) and (5), the surface potential in the 0-plane is equal to

$$\begin{aligned} \varphi_0 &= \frac{RT \ln 10}{F} (\log K_{x/y}^{\circ} - \text{pH}) \\ &\quad - \frac{RT}{F} \ln \left(\frac{\{\text{MOH}^{1-x/y}\}}{\{\text{MO}^{-x/y}\}} \right); \quad 1\text{-pK} \end{aligned} \quad (16)$$

and

$$\begin{aligned} \varphi_0 &= \frac{RT \ln 10}{F} \left(\frac{1}{2} \log K_1^{\circ} K_2^{\circ} - \text{pH} \right) \\ &\quad - \frac{RT}{2F} \ln \left(\frac{\{\text{MOH}_2^+\}}{\{\text{MO}^-\}} \right); \quad 2\text{-pK} \end{aligned} \quad (17)$$

In the case of negligible counterion association, the electrokinetic isoelectric point (pH_{iep}) coincides with the point of zero charge (pH_{pzc}) [21,23,24]. For the 1-pK model $((y-x)/x)\{\text{MOH}^{1-x/y}\} = (x/y)\{\text{MO}^{-x/y}\}$, while for 2-pK mechanism $\{\text{MOH}_2^+\} = \{\text{MO}^-\}$. This electroneutrality point (pH_{eln}), or the pristine point of zero charge, is related to the equilibrium constants of surface reactions by

$$\text{pH}_{\text{eln}} = \log K_{x/y}^{\circ} + \log \frac{y-x}{x}; \quad 1\text{-pK} \quad (18)$$

$$\text{pH}_{\text{eln}} = \frac{1}{2} \log(K_1^{\circ} K_2^{\circ}); \quad 2\text{-pK} \quad (19)$$

Accordingly,

$$\begin{aligned} \varphi_0 &= \frac{RT \ln 10}{F} (\text{pH}_{\text{eln}} - \text{pH}) \\ &\quad + \frac{RT}{F} \ln \left(\frac{\{\text{MOH}^{1-x/y}\} \{y-x\}}{\{\text{MO}^{-x/y}\} x} \right); \quad 1\text{-pK} \end{aligned} \quad (20)$$

$$\begin{aligned} \varphi_0 &= \frac{RT \ln 10}{F} (\text{pH}_{\text{eln}} - \text{pH}) - \frac{RT}{2F} \ln \left(\frac{\{\text{MOH}_2^+\}}{\{\text{MO}^-\}} \right); \quad 2\text{-pK} \end{aligned} \quad (21)$$

The point of zero potential pH_{pzp} ($\varphi_0 = 0$) may be approximated by the pH_{eln} so that the modified Nernst equation may be applied [25,26]

$$\varphi_0 = \frac{RT \ln 10}{F} (\text{pH}_{\text{eln}} - \text{pH})\alpha \quad (22)$$

where coefficient α describes deviation from the ideal behavior, for which $\alpha = 1$. For real metal oxide surfaces, the coefficient α is below 1 and depends on the kind of metal oxide [4,27,28], and also on the composition of the electrolyte solution [5].

Assumptions connected with the EIL model are essential for deducing relationships between surface charge densities and the respective electrostatic potentials. The first (inner) layer, i.e. the space between the 0- and β -planes, is commonly assumed to be a capacitor with (constant) capacitance C_1

$$C_1 = \frac{\sigma_0}{\varphi_0 - \varphi_\beta} \quad (23)$$

Capacitance C_1 is almost always expressed “per surface area” and depends on the apparent distance between the 0- and d -planes (d) and the permittivity of the medium (ε)

$$C_1 = \frac{\varepsilon}{d} \quad (24)$$

The second (outer) layer, i.e. the space between the β - and d -plane, is sometimes assumed to be a second capacitor with capacitance C_2

$$C_2 = \frac{\sigma_\beta}{\varphi_d - \varphi_\beta} \quad (25)$$

The Gouy–Chapman theory provides the relationship between the surface charge density of the diffuse layer σ_d and the potential at the onset of the diffuse layer φ_d

$$\sigma_d = -\sigma_s = -\sqrt{8RT\varepsilon I_c} \sinh\left(\frac{-F\varphi_d}{RT}\right) \quad (26)$$

where I_c is the ionic strength and ε is the permittivity of the medium. According to the same theory, the potential drop within the hydrodynamically stagnant part of the diffuse layer, i.e. between the d -plane and the electrokinetic s -plane, is given by

$$\varphi_d = \frac{2RT}{F} \ln\left(\frac{\exp(-\kappa s) + \text{th}(F\zeta/4RT)}{\exp(-\kappa s) - \text{th}(F\zeta/4RT)}\right) \quad (27)$$

where s is the separation distance of the electrokinetic s -plane from the d -plane, and κ is the Debye–Hückel parameter given by

$$\kappa = \sqrt{\frac{2I_c F^2}{\varepsilon RT}} \quad (28)$$

The general model of EIL may be simplified to the Triple Layer Model (TLM) or to the Double Layer Model (DLM). Both approximations take into account that potential φ_β should be higher in magnitude compared to the electrokinetic ζ -potential. However, they differ in the value of φ_d . TLM assumes that the onset of the diffuse layer corresponds to the electrokinetic slip plane so that $s \approx 0$ and $\varphi_d \approx \zeta$. The requirement $|\varphi_\beta| > |\zeta|$ is

satisfied by assuming a significant potential drop in the outer layer $|\varphi_\beta| > |\varphi_d|$, which corresponds to $C_2 \ll \infty$. DLM assumes that the onset of the diffuse layer corresponds to the β -plane, i.e. $\varphi_\beta \approx \varphi_d$, which corresponds to $C_2 \approx \infty$. The requirement $|\varphi_\beta| > |\zeta|$ is satisfied by assuming a significant shift of the electrokinetic plane from the onset of the diffuse layer, which corresponds to $s > 0$ and $C_2 \approx \infty$.

3. Experimental and results

3.1. Materials

All solutions were prepared using redistilled and decarbonized water: NaClO_4 (p.a., Fluka), NaCl (p.a., Fluka), HClO_4 (70% solution, Merck), HCl (0.1 mol dm^{-3} , titrival, Fluka), NaOH (0.1 mol dm^{-3} , titrival, Fluka), standard buffers (Fluka), TiO_2 particles (P-25, Degussa; 60% anatase, 40% rutile [29] of specific surface area: 50 g m^{-2} ; the sample was purified by extended washing). The anatase single crystal electrode was prepared using the mineral anatase from Hardangervidda (Norway) and is shown in Fig. 1.

3.2. Methods

Anatase surface potential was measured in aqueous sodium perchlorate and sodium chloride solutions. The pH was varied by adding NaOH and HClO_4 (or HCl in the case of sodium chloride solution) and measured with a glass electrode (Metrohm, 6.0222.100). Reference silver/silver chloride electrode was used with a salt bridge (Metrohm, 6.0233.100) filled with the same electrolyte solution as in the measuring system. The glass electrode was calibrated with five standard buffers. During measurements, the system was thermostated at 25°C and kept under an argon atmosphere.

Electromotivities E (“electromotive force” [7]) of the cells:

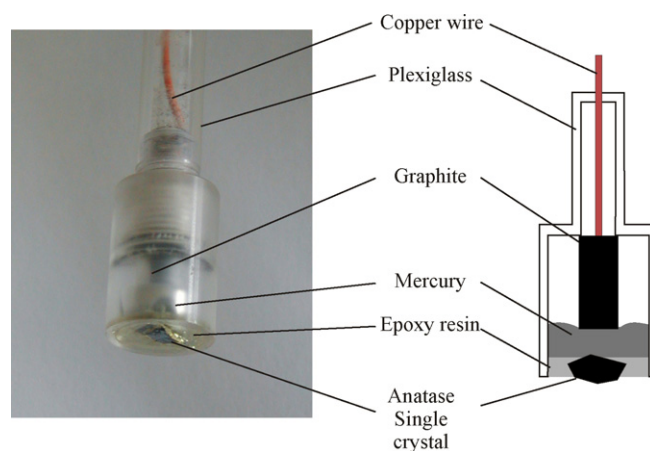
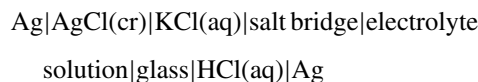


Fig. 1. Anatase single crystal electrode.

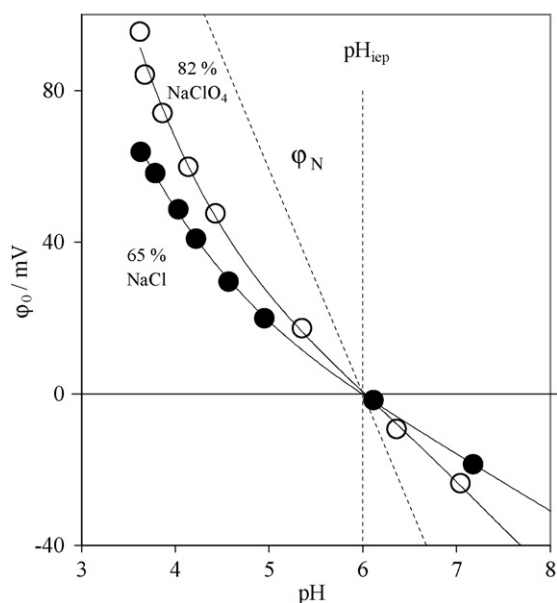
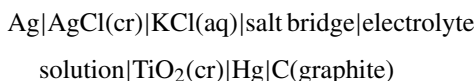


Fig. 2. The effect of sodium perchlorate (open circles) and sodium chloride (full circles) on the surface potential of anatase as a function of pH at 25 °C. $I_c = 10^{-3} \text{ mol dm}^{-3}$. Dashed line represents the Nernstian potential φ_N and was drawn through the point of zero potential.

and



were measured with two pH-meters (713 Metrohm).

Surface charge density σ_0 was obtained by acid base potentiometric titration [30] of the colloid suspensions of TiO_2 particles ($\gamma \approx 16 \text{ g dm}^{-3}$). Values of σ_0 were calculated from the potentiometric titration curves by a standard procedure [31].

The electrokinetic ζ -potential was measured using the Zeta-sizer 3000 Standard (Malvern) based on the laser-Doppler microelectrophoresis technique. TiO_2 dispersion was prepared by adding a small amount of powder to the aqueous solution ($\gamma \approx 100 \text{ mg dm}^{-3}$).

3.3. Results

Surface potentials were evaluated from the electromotivity data by setting the point of zero potential at the measured isoelectric point, $\text{pH}_{\text{iep}} 6.1$. Surface potentials, as a function of pH, for NaClO_4 and NaCl ($I_c = 0.001 \text{ mol dm}^{-3}$) are shown in Fig. 2. Appreciable reproducibility of data was obtained in the acidic region. In neutral and basic regions, the potentials were not stable and changed with time, which could be explained by slow equilibration causing hysteresis [6,32]. As expected [5,3,26,28], the slopes were lower in magnitude than the Nernstian; in the acidic region, approximately 82% for sodium perchlorate, and 65% for sodium chloride.

Values of the surface charge density in the 0-plane (σ_0) are shown in Fig. 3, while electrokinetic potentials of TiO_2 particles, as a function of pH, are displayed in Fig. 4. The isoelectric point of TiO_2 particles at $I_c = 10^{-3} \text{ mol dm}^{-3}$ was found at $\text{pH}_{\text{iep}} 6.1$.

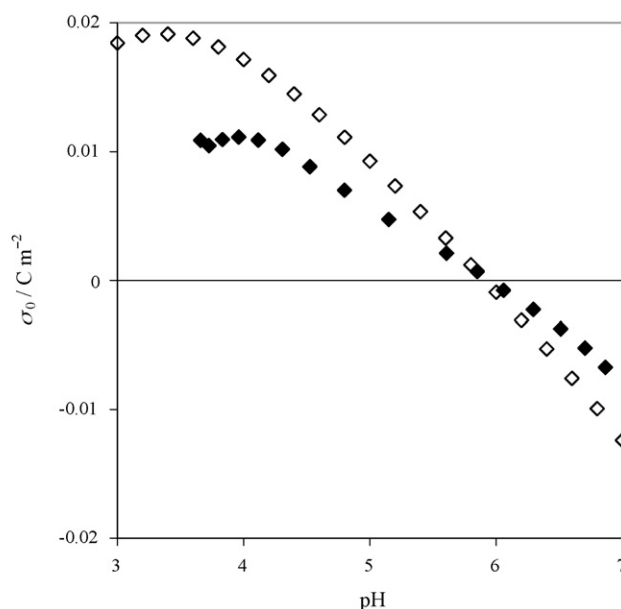


Fig. 3. The effect of sodium perchlorate (open diamonds) and sodium chloride (full diamonds) on surface charge densities of TiO_2 as a function of pH at 25 °C. $I_c = 10^{-3} \text{ mol dm}^{-3}$.

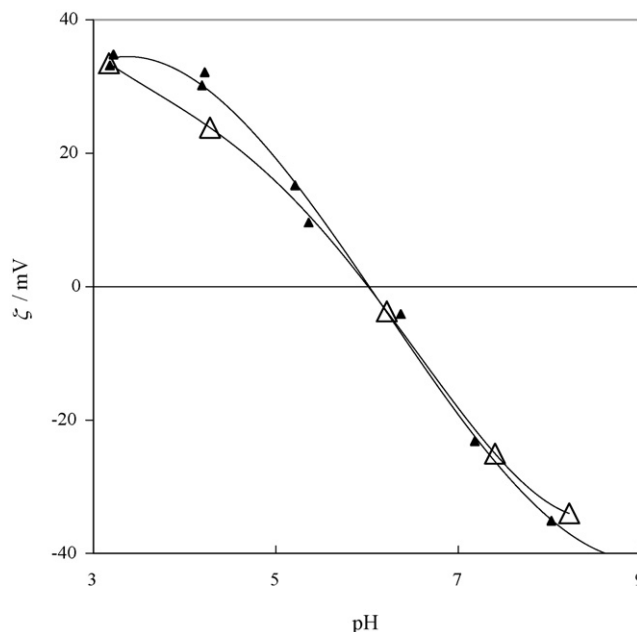


Fig. 4. Electrokinetic ζ -potential of TiO_2 as a function of pH in aqueous NaClO_4 (open triangles) and NaCl (full triangles) solutions at 25 °C. $I_c = 10^{-3} \text{ mol dm}^{-3}$.

As expected, the values of zeta potentials are significantly lower in magnitude than the measured surface potentials.

4. Data interpretation

Data obtained in sodium perchlorate and sodium chloride solutions were interpreted on the basis of the Surface Complexation Model assuming 1-pK (Eqs. (1)–(3)) and 2-pK mechanisms (Eqs. (4)–(7)) of surface protonation reactions. For the 1-pK mechanism of surface charging, the values of $x = 1$ and $y = 3$ were

used, as commonly accepted for anatase [17,18,22]. Accordingly, the surface species for anatase are $\text{MOH}^{-1/3}$ and $\text{MO}^{+2/3}$.

The potential at the onset of the diffuse layer φ_d was calculated from electrokinetic data via Eq. (27) assuming the electrokinetic slip plane separation of 10 \AA [33]. Calculations were also performed by taking the slip plane separation of 5 and 15 \AA , but did not show a significant difference. Within the double layer approximation, the potential at the β -plane is assumed to be equal to φ_d ($\varphi_\beta = \varphi_d$). The capacitance of the inner layer capacitor C_1 was calculated by Eq. (23) using the measured σ_0 and φ_0 values, and φ_d values as obtained from electrokinetic data. The net surface charge density (σ_s) was calculated from φ_d values using Eq. (26). The ratios of surface concentrations of positively and negatively charged surface species were calculated from the measured surface potentials. For the 1-pK mechanism, the ratio $\{\text{MOH}^{2/3}\}/\{\text{MO}^{-1/3}\}$ was calculated using Eq. (20), while for the 2-pK mechanism, the ratio $\{\text{MOH}_2^+\}/\{\text{MO}^-\}$ was calculated by Eq. (21). The differences between surface concentrations of positively and negatively charged surface species were calculated from the net surface charge density σ_s using Eqs. (14) and (15), for 1-pK and 2-pK mechanisms, respectively. Individual values of surface concentrations of positive and negative surface sites were obtained from the known difference and ratio. Surface concentrations of associated perchlorate ions were calculated by Eqs. (10) and (11) using the measured σ_0 values and known values of surface concentrations of positive and negative sites. The surface concentration of uncharged MOH species (only for the 2-pK mechanism) was obtained by subtracting surface concentrations of $\{\text{MOH}_2^+\}$, $\{\text{MO}^-\}$ and $\{\text{MOH}_2^+\cdot\text{ClO}_4^-\}$, or $\{\text{MOH}_2^+\cdot\text{Cl}^-\}$, from Γ_{tot} taken as $1.5 \times 10^{-5} \text{ mol m}^{-2}$ (Eq. (9)). Influence of different

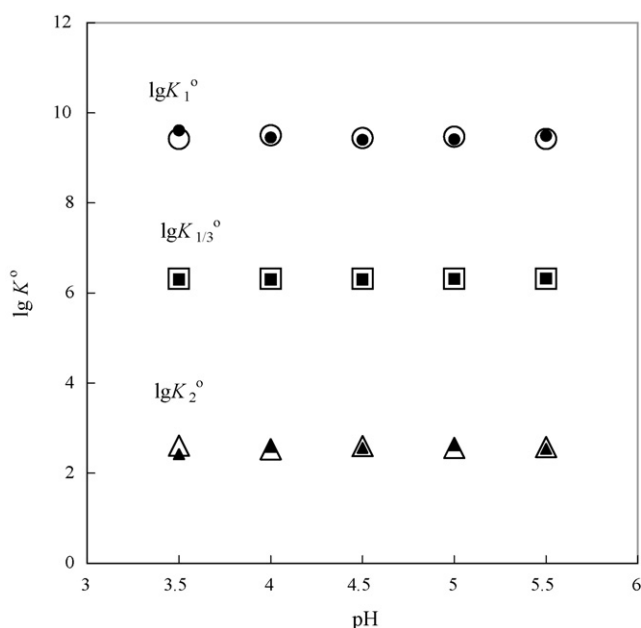


Fig. 5. Thermodynamic equilibrium constants of surface protonation at TiO_2 aqueous interface at 25°C and $I_c = 10^{-3} \text{ mol dm}^{-3}$. Open symbols correspond to NaClO_4 and full symbols to NaCl ; squares refer to the equilibrium constant of the 1-pK mechanism surface reaction ($\lg K_{1/3}^0$), while circles ($\lg K_1^0$) and triangles ($\lg K_2^0$) refer to the 2-pK mechanism of surface reactions.

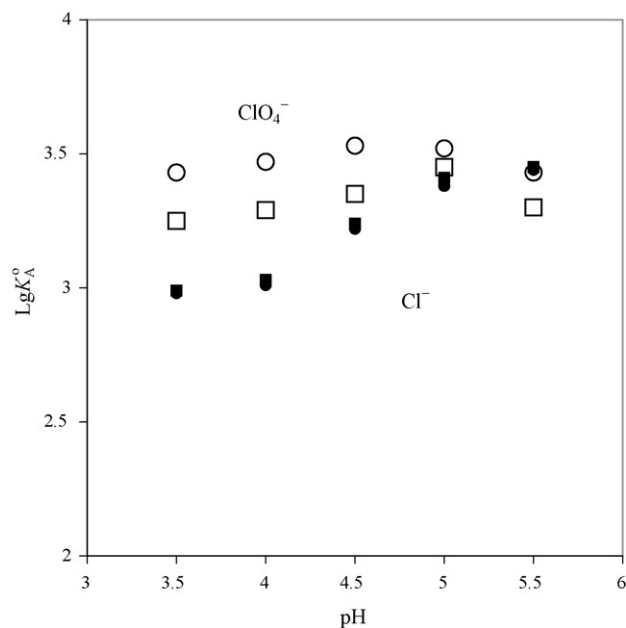


Fig. 6. Thermodynamic equilibrium constants for association of counterions with oppositely charged surface sites at TiO_2 aqueous interface at 25°C and $I_c = 10^{-3} \text{ mol dm}^{-3}$. Open symbols refer to association of ClO_4^- ($\lg K_{\text{ClO}_4^-}^0$): (□) 1-pK and (○) 2-pK model. Equilibrium constants for association of Cl^- ions ($\lg K_{\text{Cl}^-}^0$): (■) 1-pK and (●) 2-pK models (overlap of data points).

values of Γ_{tot} was examined but without significant effect on the results.

The described procedure enabled us to obtain individual values of surface concentrations of all active species at the interface for each pH value. Thermodynamic equilibrium constants of surface protonation and of counterion association with oppositely charged surface groups were calculated by Eqs. (1)–(7) using known values of surface concentrations and surface potentials. Calculations were performed for the acidic region, and the results are presented in Figs. 5 and 6.

Values of the electrical capacitance C_1 were calculated from surface charge densities (σ_0) and the respective electrostatic potentials (φ_0 and φ_β) via Eq. (23) and are displayed in Fig. 7.

5. Discussion

Simultaneous measurements of the surface potential, surface charge and electrokinetic potential enabled evaluation of surface concentrations of all interfacial species and thus calculation of parameters, such as surface equilibrium constants and capacitance. It is clear that the values of thermodynamic surface protonation equilibrium constants should not depend on the composition of the solution. Indeed, as shown in Fig. 5, these constants do not depend on pH and are practically the same for sodium chloride and perchlorate, despite the fact that these two ions affect the surface potential and charge differently (Figs. 2 and 3). Unfortunately, this applies to both assumed mechanisms of surface charging, so this result cannot be used to distinguish between them and choose the proper one. The thermodynamic protonation equilibrium constants, corresponding to the 2-pK mechanism, obtained in this work from the surface

Table 1
Summary of data for TiO₂ aqueous interface. Equilibrium constants of surface reaction according to 1-pK and 2-pK models and electrical capacitance C_1 are presented

Reference	Method	$\lg K_1^0$	$\lg K_2^0$	$\lg K_{1/3}^0$	$\lg K_{Cl^-}^0$	$\lg K_{ClO_4^-}^0$	C_1 (F m ⁻²)
This article	$\varphi_0, \sigma_0, \zeta$	9.5	2.5	6.2	3.0–3.4	3.45	0.3–1.5 pH-dependent
[35–37]	σ_0	9.2	2.6		4.3	4.3	
[38]	σ_0, Γ_{ads}	8.9	3.1		3.1		
[39,40]	σ_0, Γ_{ads}	8.8	3.4			4.3	
[26]	σ_0	8.9	2.7				
[41]	Born solvation theory	8.4	2.0				
[42]	σ_0	9.2 (anatase) 9.0 (rutile)	2.8 (anatase) 2.6 (rutile)		2.6 (anatase) 1.9 (rutile)	1.3 (anatase) 1.45 (rutile)	
[43]	σ_0, ζ	6.4	3.5				
[44]				6.72			

potential, surface charge and electrokinetic potential data, are $\lg K_1^0 = 9.5$ and $\lg K_2^0 = 2.5$. They agree well with the literature data as seen from Table 1.

The thermodynamic equilibrium constants for association of perchlorate and chloride ions with positively charged surface groups are displayed in Fig. 6 and in Table 1. Their values do not depend significantly on pH for perchlorate ions and are slightly lower for the 1-pK mechanism. For the 2-pK model, $\lg K_{A1}^0(ClO_4^-) = 3.5$ was obtained, which is significantly higher than the values obtained by Janusz et al. [39,40] and Berube and De Bruyn [35,36]. The results obtained with chloride ions are somewhat different. The calculated points are the same for both 1-pK and 2-pK models but an increase in the equilibrium constant was found at pH 4.5. The values lie in the range $\lg K_{A1}^0(Cl^-) = 3.0$ –3.4.

The calculated values of capacitances C_1 do not depend on the employed model (Fig. 7). They increase with pH, which is more pronounced in the case of perchlorate ions. It should be noted that in the course of the calculation procedure, errors due to

uncertainty of the experimental data propagate and so the results on the counterion association equilibrium constants and capacitances are less reliable. However, one may still conclude that the obtained values of capacitance C_1 are in the expected range [1,34,37,42] and that the assumption of their constancy is just an approximation introduced by necessity. In view of Eq. (24), one might speculate that the permittivity of the inner Helmholtz layer decreases with the surface potential, but such a simplification cannot provide a proper answer. It is interesting that perchlorate and chloride ions affect the interfacial equilibrium in different ways; in the perchlorate medium, surface potentials and surface charge densities are higher while electrokinetic potentials are slightly lower, which is due to the difference in their association equilibrium constants and capacitances of the inner Helmholtz layer. The simple Bjerrum concept [14,15] would suggest that effectively smaller ions may approach the central surface charged group closer, resulting in higher values of both the association equilibrium constant and the capacitance. However, such approach neglects the effect of the possible change of hydration of the ionic species.

The potential of the applied method and the procedure lies primarily in determination of the surface protonation equilibrium constants. The only assumption made in the calculation was the choice of the total density of active surface sites, Γ_{tot} . The value of $\Gamma_{tot} = 1.5 \times 10^{-5} \text{ mol m}^{-2}$ was taken from literature [43]. Increasing the Γ_{tot} value in calculation (from 0.5×10^{-5} to $10 \times 10^{-5} \text{ mol m}^{-2}$) results in lower values of K_1 ($\lg K_1 = 9.7$ –9.1), and consequently in lower K_2 values, but both equilibrium constants remain pH independent. Changing the Γ_{tot} value has no significant influence on the calculated C_1 value.

The advantage of simultaneous interpretation of different sets of data is that one avoids the common assumption of the constancy of parameters describing the interfacial equilibrium, so one is able to test different theoretical models.

6. Conclusions

Construction of anatase single crystal electrode enables evaluation of inner surface potential at anatase/electrolyte interface. The magnitude of the slope of $\varphi_0(\text{pH})$ function was found to be lower than the Nernstian, which is consistent with the Surface Complexation Model. Simultaneous measurements of surface potential, surface charge density and electrokinetic potential

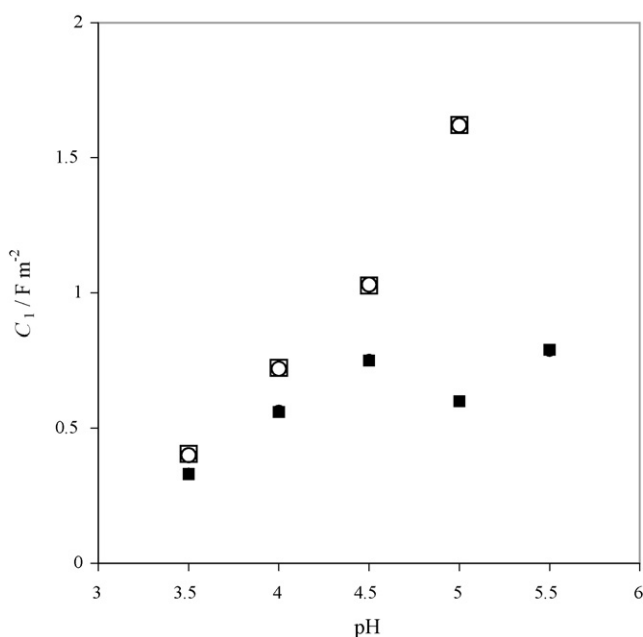


Fig. 7. Capacitance of the first (inner) layer capacitor C_1 at TiO₂ aqueous interface at 25 °C and $I_c = 10^{-3} \text{ mol dm}^{-3}$. Open symbols refer to association of ClO₄⁻: (□) 1-pK and (○) 2-pK model, while association of Cl⁻ is calculated for: (■) 1-pK and (●) 2-pK models (overlap of data points).

enabled evaluation of surface concentrations of all interfacial species and thus calculation of parameters, such as surface equilibrium constants and capacitance of the inner layer. The values of thermodynamic surface protonation equilibrium constants for first and second step of protonation were found to be independent on the composition of the solution, i.e. on pH and the kind of counterions, despite the fact that chloride and perchlorate ions affect the surface potential and charge differently. The applied procedure avoids the assumption on the constant capacitance of the inner layer capacitor which was found to depend significantly on pH.

References

- [1] J. Lyklema, *Fundamentals of Interface and Colloid Science, Solid–Liquid Interface*, vols. I–II, Academic Press, London, 1995.
- [2] N. Kallay, T. Preočanin, S. Žalac, *Langmuir* 20 (2004) 2986.
- [3] N. Kallay, D. Čakara, *J. Colloid Interface Sci.* 232 (2000) 81.
- [4] N. Kallay, A. Čop, E. Chibowski, L. Holysz, *J. Colloid Interface Sci.* 259 (2003) 89.
- [5] N. Kallay, Z. Dojnović, A. Čop, *J. Colloid Interface Sci.* 286 (2005) 610.
- [6] T. Preočanin, A. Čop, N. Kallay, *J. Colloid Interface Sci.* 299 (2006) 772–776.
- [7] V.L. Simeon, *Chem. Int.* 26 (6) (2004) 12.
- [8] A.V. Delgado, F. Gonzalez-Caballero, R.J. Hunter, L.K. Koopal, J. Lyklema, *Pure Appl. Chem.* 77 (2005) 1753.
- [9] N. Kallay, T. Preočanin, S. Žalac, H. Lewandowski, H.D. Narres, *J. Colloid Interface Sci.* 211 (1999) 401.
- [10] J. Westall, H. Hohl, *Adv. Colloid Interface Sci.* 12 (1980) 265.
- [11] R. Sprycha, *J. Colloid Interface Sci.* 102 (1984) 173.
- [12] R. Charmas, P. Zarzycki, F. Villieras, F. Thomas, B. Prélot, W. Piasecki, *Colloids Surf. A* 244 (2004) 9.
- [13] J. Lützenkirchen, *J. Colloid Interface Sci.* 217 (1999) 8.
- [14] N. Kallay, M. Tomić, *Langmuir* 4 (1988) 559.
- [15] M. Tomić, N. Kallay, *Langmuir* 4 (1988) 565.
- [16] W.H. van Riemsdijk, G.H. Bolt, L.K. Koopal, J. Blaakmeer, *J. Colloid Interface Sci.* 109 (1986) 219.
- [17] R.H. Yoon, T. Salma, G. Donnay, *J. Colloid Interface Sci.* 70 (1979) 483.
- [18] T. Hiemstra, P. Venema, W.H. Van Riemsdijk, *J. Colloid Interface Sci.* 184 (1996) 680.
- [19] D.E. Yates, S. Levine, T.W. Healy, *J. Chem. Soc. Faraday Trans. 1* 70 (1974) 1807.
- [20] W. Rudzinski, R. Charmas, W. Piasecki, J.M. Cases, M. Francois, F. Villieras, L.J. Michot, *Colloid Surf. A* 137 (1998) 57.
- [21] J. Lützenkirchen, P. Magnico, *Colloids Surf. A* 137 (1998) 345.
- [22] T. Hiemstra, J.C.M. De Wit, W.H. Van Riemsdijk, *J. Colloid Interface Sci.* 133 (1989) 105.
- [23] M.A. Pyman, J.W. Bowden, A.M. Posner, *Aust. J. Soil Res.* 17 (1979) 191.
- [24] J. Lyklema, *J. Colloid Interface Sci.* 99 (1984) 109.
- [25] T.W. Healy, D.E. Yates, L.R. White, D. Chan, *J. Electroanal. Chem.* 80 (1977) 57.
- [26] H. Van der Vlekkert, L. Bousse, N. De Rooij, *J. Colloid Interface Sci.* 122 (1988) 336.
- [27] N. Kallay, R. Sprycha, M. Tomić, S. Žalac, Ž. Torbić, *Croat. Chem. Acta* 63 (1990) 467.
- [28] M.J. Avena, O.R. Camara, C.P. De Pauli, *Colloids Surf. A* 69 (1993) 217.
- [29] A. Foissy, A. M'Pandou, J.M. Lamarche, N. Jaffrezic-Renault, *Colloids Surf. A* 5 (1982) 363.
- [30] H. Kita, N. Henmi, K. Shimazu, H. Hattori, K. Tanabe, *J. Chem. Faraday Trans. 1* 77 (1981) 2451.
- [31] P. Hesleitner, D. Babić, N. Kallay, E. Matijević, *Langmuir* 3 (1987) 815.
- [32] W. Piasecki, *Langmuir* 19 (2003) 9526.
- [33] M. Čolić, D.W. Fuerstenau, N. Kallay, E. Matijević, *Colloids Surf. A* 59 (1991) 169.
- [34] J. Lützenkirchen, P. Magnico, P. Behra, *J. Colloid Interface Sci.* 170 (1995) 326.
- [35] Y.G. Berube, P.L. De Bruyn, *J. Colloid Interface Sci.* 28 (1968) 92.
- [36] Y.G. Berube, P.L. De Bruyn, *J. Colloid Interface Sci.* 27 (1968) 305.
- [37] R.O. James, G.A. Parks, in: E. Matijević (Ed.), *Surface and Colloid Science*, 12, Wiley-Interscience, New York, 1982, p. 119.
- [38] R. Sprycha, J. Szczypa, *J. Colloid Interface Sci.* 102 (1984) 173–185.
- [39] W. Janusz, A. Sworska, J. Szczypa, *Colloids Surf. A* 152 (1999) 223.
- [40] W. Janusz, *Pol. J. Chem.* 65 (1991) 799.
- [41] D.A. Sverjensky, N. Sahai, *Geochim. Cosmochim. Acta* 60 (1996) 3773.
- [42] N. Sahai, D.A. Sverjensky, *Geochim. Cosmochim. Acta* 61 (1997) 2801.
- [43] N. Kallay, D. Babić, E. Matijević, *Colloids Surf. A* 19 (1986) 375.
- [44] M.L. Machesky, D.J. Wesolowski, D.A. Plamer, M.K. Ridley, *J. Colloid Interface Sci.* 239 (2001) 314.